RSC Advances

PAPER

View Article Online
View Journal | View Issue

Cite this: *RSC Adv.*, 2024, **14**, 39779

Blue light-activated 5,10,15,20-tetrakis(4-bromophenyl)porphyrin for photodynamic eradication of drug-resistant *Staphylococcus aureus*†

Hongshuang Qin,[a] Huaying Niu,[a] Yanxiang Guo,[a] Xiaoting Wang,[a] Tao Liu*[c] and Chuanqi Zhao*[b]

Photodynamic therapy (PDT) has emerged as an effective way to deal with drug-resistant bacterial infections. Especially, blue light (BL) mediated PDT (BL-PDT) presents unique advantages in the treatments of skin infection due to the strong light absorption of superficial skin, weak penetration of BL and little damage to deep tissues. However, the photosensitizers used for BL-PDT are very limited, and the ongoing development of novel BL photosensitizers is indispensable. Porphyrins are good sources for developing efficient photosensitizers. Herein, for developing more effective BL photosensitizers, five porphyrin derivatives that can be excited by BL [5,10,15,20-tetraphenylporphyrin (TPP), 5,10,15,20-tetrakis(4-bromophenyl)porphyrin (TBPP), 5,10,15,20-tetrakis(4-chlorophenyl)porphyrin (TCPP), 5,10,15,20-tetrakis(4-fluorophenyl)porphyrin (TFPP), 5,10,15,20-tetrakis(4-iodophenyl)porphyrin (TIPP)] are subjected to the investigation of PDT against MRSA (methicillin resistant *Staphylococcus aureus*). The results reveal that TBPP-mediated BL-PDT shows outstanding bactericidal effects. Mechanism studies show that TBPP + BL can induce reactive oxygen species (ROS) up-regulated in MRSA, rupture cell membrane, inhibit ATP (adenosine triphosphate) production and virulence factor expression. Furthermore, TBPP + BL effectively eliminates MRSA form biofilms, inhibits biofilm formation and disintegrates mature biofilms. More importantly, TBPP-PDT significantly accelerate mouse skin wound healing in a biofilm infection model. Our work offers new insights into the development of novel BL photosensitizers.

Received 27th October 2024
Accepted 9th December 2024

DOI: 10.1039/d4ra07666d

rsc.li/rsc-advances

1 Introduction

In recent years, bacteria have developed severe resistance to antibiotics due to the antibiotic overuse and misuse.[1,2] In medicine and health fields, more and more infectious diseases like pneumonia and diarrhea are becoming harder to treat.[3,4] In accordance with World Health Organization, virtually all the pathogenic microorganisms that lead to infective deaths exhibit antibiotic resistance.[5–7] To address the growing problem of antimicrobial resistance, more new antibacterial therapeutic methods need to be developed.[8,9] In addition to the development of new antibacterial drugs and biocides, it is absolutely necessary to focus on other antimicrobial methods.[10–12]

Photodynamic therapy (PDT), an advanced optical technology, has attracted extensive attention in the fields of medicine and public health.[13,14] PDT utilizes light sources, light-sensitive photosensitizers and available oxygen to generate reactive oxygen species (ROS).[15,16] The cytotoxic ROS generated during PDT reacts with various bacterial components, resulting in biomacromolecule inactivation and cell death.[17,18] The nonselective and fast-acting properties of ROS minimize the development of bacterial resistance.[19,20] In particular, blue light (BL, 400–495 nm) mediated PDT (BL-PDT) presents fascinating advantages in skin infection treatments.[21,22] Owing to the strong light absorption of superficial tissues, BL-PDT has good effects in treatments of skin infection. More importantly, BL-PDT avoids damage to deep healthy tissues due to its shallow penetration depth.[23–26] However, blue light photosensitizers used for antimicrobial treatments are still limited, and the ongoing development of novel blue light photosensitizers is essential.

[a]*Department of Biological and Food Engineering, Lyuliang University, Lvliang, Shanxi 033001, China*

[b]*Laboratory of Chemical Biology, State Key Laboratory of Rare Earth Resource Utilization, Changchun Institute of Applied Chemistry, Chinese Academy of Sciences, Changchun, Jilin 130022, China. E-mail: zhaocq@ciac.ac.cn*

[c]*Department of Chemistry and Chemical Engineering, Lyuliang University, Lvliang, Shanxi 033001, China. E-mail: liutao@llu.edu.cn*

† Electronic supplementary information (ESI) available. See DOI: https://doi.org/10.1039/d4ra07666d

Porphyrins are an important class of photosensitizers. Porphyrins exhibit good photodynamic activities, and many porphyrins have been approved for clinical photodynamic therapy, such as photofrin, foscan, NPe6, levulan and metvix.[27,28] Porphyrin derivatives are good sources for developing novel and efficient photosensitizers. In this study, in order to find more effective BL photosensitizers for the treatments of drug-resistant bacteria, for the first time, porphyrin derivatives 5,10,15,20-tetraphenylporphyrin (TPP), 5,10,15,20-tetrakis(4-bromophenyl)porphyrin (TBPP), 5,10,15,20-tetrakis(4-chlorophenyl)porphyrin (TCPP), 5,10,15,20-tetrakis(4-fluorophenyl)porphyrin (TFPP) and 5,10,15,20-tetrakis(4-iodophenyl)porphyrin (TIPP) (Fig. 1), which can be excited by blue light,[29–32] were investigated for photodynamic bactericidal effects against methicillin-resistant *Staphylococcus aureus* (MRSA). MRSA were chosen because they are the main pathogens causing serious infectious diseases with high mortality rates.[33]

Our results showed that the PDT mediated by the five compounds (TPP-PDT, TBPP-PDT, TCPP-PDT, TFPP-PDT, TIPP-PDT) all had the antibacterial effects on MRSA. Among them, TBPP-PDT exhibited the best bactericidal activity. Thus, we focused attention on the germicidal effects of TBPP-PDT. Mechanism studies showed that TBPP-PDT could induce ROS overexpression in MRSA, destroy bacterial cell membrane integrity, inhibit ATP (adenosine triphosphate) synthesis and virulence factor expression. Further results showed that TBPP-PDT effectively inhibited biofilm formation, killed MRSA wrapped in biofilms and dissolved mature biofilms. More importantly, TBPP-PDT could obliterate the biofilms on the skin wounds of mice, reduce inflammation and accelerate wound healing. Our work provides new insights into the development of novel BL photosensitizers for the treatments of drug-resistant bacterial infections.

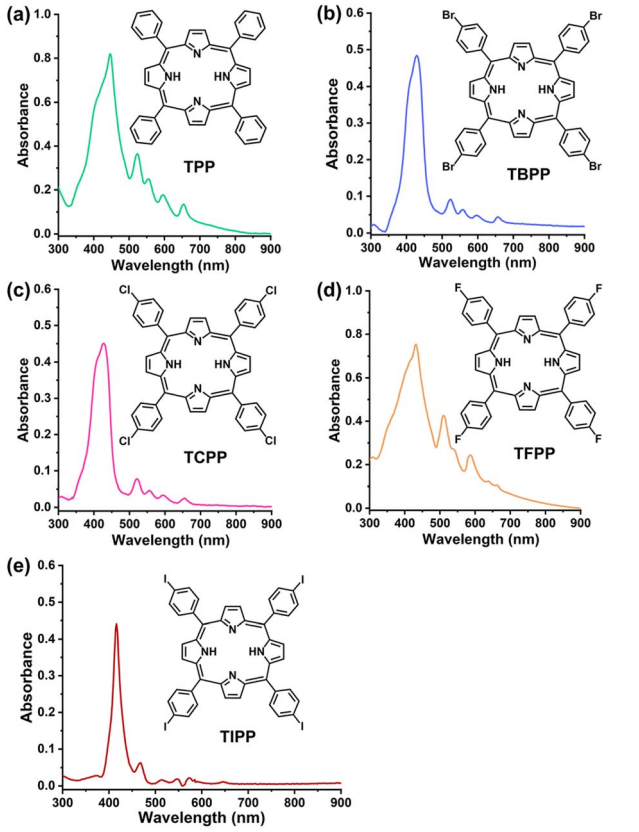

Fig. 1 (a–e) Chemical structures and UV-Vis spectra of TPP, TBPP, TCPP, TFPP, TIPP (20 μM) in PBS. TPP, 5,10,15,20-tetraphenyl porphyrin. TBPP, 5,10,15,20-tetrakis(4-bromophenyl)porphyrin. TCPP, 5,10,15,20-tetrakis(4-chlorophenyl)porphyrin. TFPP, 5,10,15,20-tetrakis(4-fluorophenyl)porphyrin. TIPP, 5,10,15,20-tetrakis(4-iodophenyl) porphyrin.

2 Results

2.1 Antibacterial activity analysis of TPP-PDT, TBPP-PDT, TCPP-PDT, TFPP-PDT and TIPP-PDT

The UV-Vis spectra of the 5 compounds (TPP, TBPP, TCPP, TFPP, TIPP) were provided in Fig. 1. The compounds were assessed for photodynamic antibacterial activities against MRSA (methicillin-resistant *Staphylococcus aureus*, ATCC43300) by colony counting assay. The MRSA suspensions containing different concentrations of compounds were irradiated with blue light (BL, 120 J cm^{-2}), and the survival bacteria were detected. The MRSA treated with compounds alone (no light)

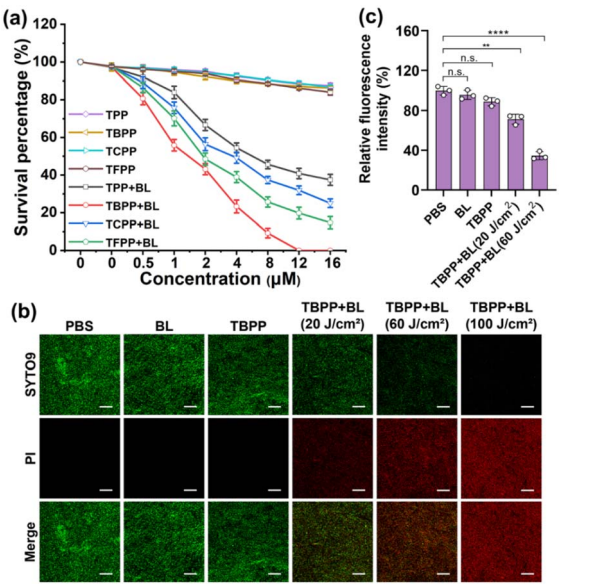

Fig. 2 TBPP-PDT exhibited bactericidal activities against MRSA and induced the damage of cell membranes. (a) The viability of MRSA incubated with different concentrations (0, 0.5, 1, 2, 4, 8, 12, 16 μM) of compounds for 20 min followed by irradiation at 120 J cm^{-2} with blue light (445 nm) (mean ± SD, $n = 3$). (b) SYTO9/PI staining images of MRSA incubated with TBPP (12 μM) for 20 min and irradiated with different doses of light (0, 20, 60, 100 J cm^{-2}) with an excitation of 445 nm using confocal microscopy. PI, propidium iodide. Red and green signals indicate the dead and living bacteria. Scale bar = 20 μm. (c) The membrane potentials of MRSA incubated with 12 μM TBPP for 20 min and irradiated with different doses of light (0, 20, 60 J cm^{-2}) (mean ± SD, $n = 3$). $^{**}P < 0.01$, $^{****}P < 0.0001$ (two-way ANOVA, Dunnett's *posthoc* test). PDT, photodynamic therapy. BL, blue light. MRSA, methicillin-resistant *Staphylococcus aureus*.

were used as the controls. As shown in Fig. 2a and S1,† the PDT mediated by the five compounds (TPP-PDT, TBPP-PDT, TCPP-PDT, TFPP-PDT, TIPP-PDT) all could inhibit MRSA vitality, and TBPP-PDT showed the best inhibitory effects with the complete inhibition of bacterial vitality at 12 μM of TBPP. The minimal bactericidal concentration (MBC) of PDT mediated by the five compounds was shown in Table S1.† Therefore, in the subsequent studies, we focused on the photodynamic bactericidal activity of TBPP.

The relationship between survival percentage and light dose during TBPP-PDT was measured. As shown in Fig. S2,† with the rising of light dose, the survival of MRSA steadily decreased. When the irradiation dose reached 100 J cm^{-2}, MRSA vitality was completely inhibited. Moreover, TBPP exhibited relatively good stability (Fig. S3†). In addition, TBPP-PDT exhibited remarkable bactericidal effects against *Pseudomonas aeruginosa* (*P. aeruginosa*, Gram-negative bacteria) and *Candida albicans* (*C. albicans*, pathogenic fungi) (Fig. S4†).

To further verify the bactericidal effects of TBPP-PDT against MRSA, the live/dead bacteria assay (SYTO9/PI staining) was carried out. SYTO9 is capable of traversing intact bacterial cell membranes and stain live bacteria green, whereas PI (propidium iodide) is only able to pass through incomplete cell membranes, labeling dead bacteria red.[34] MRSA were exposed to TBPP, irradiated with blue light, and stained by SYTO9 as well as PI. As shown in Fig. 2b, slight red fluorescence was found in the groups treated with PBS, BL alone and TBPP alone. However, obvious red fluorescence appeared in MRSA treated with TBPP + BL. Furthermore, with the increase of light dose, the red fluorescence was gradually enhanced. These results confirmed that MRSA were destroyed by the treatments of TBPP + BL. Moreover, the PI staining of MRSA indicated the damage of cell membranes. Besides, the fluorescence intensity of membrane potential probe DiBAC4(3) [bis-(1,3-dibutylbarbituric acid)-trimethine oxonol] was observably decreased after treatments with TBPP + BL (Fig. 2c), suggesting the disruption of MRSA cell membranes.

2.2 Bactericidal mechanism analysis of TBPP-PDT

In addition to the reactive oxygen species (ROS) produced by TBPP-PDT outside bacterial cells, the ROS that caused cell membrane damage may also include the ROS generated by TBPP + BL inside bacteria. Therefore, we investigated whether TBPP could enter the bacteria. As shown in the Fig. S5 and S6,† the fluorescence of TBPP could be detected in MRSA after incubation, indicating the uptake of TBPP by MRSA. Then ROS generation in MRSA was evaluated using 2′,7′-dichlorodihydrofluorescein diacetate (DCFH-DA) probe. As shown in Fig. 3a and S7,† a large amount of ROS could be detected in MRSA after treatments of TBPP + BL, suggesting that TBPP could be internalized by MRSA and generated ROS in bacteria under blue light. To identify ROS types produced by TBPP + BL, four main types [superoxide anion ($O_2^{\bullet -}$), singlet oxygen ($^1O_2$), hydrogen peroxide (H_2O_2), hydroxyl radical (OH^-)] of ROS were tested. As shown in Fig. 3b–e, after TBPP + BL treatments, singlet oxygen level increased obviously, whereas no remarkable changes were

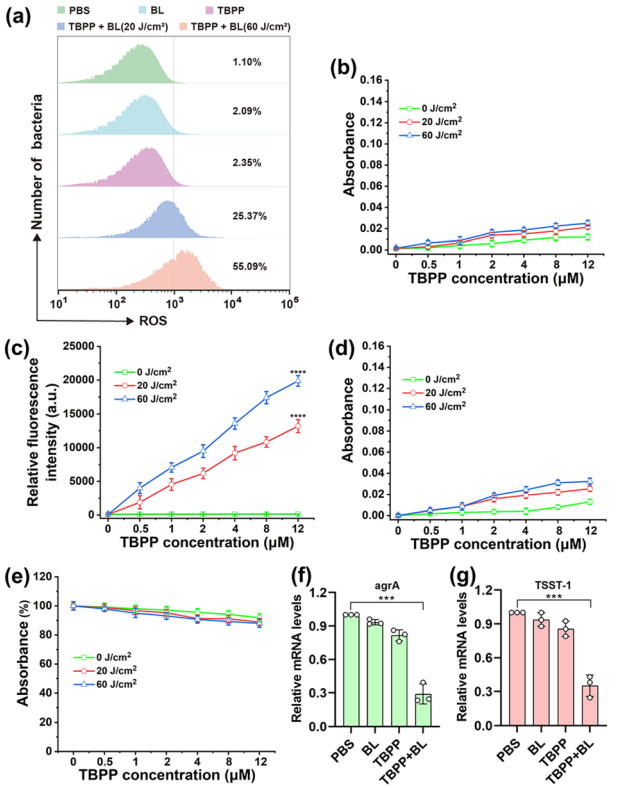

Fig. 3 TBPP-PDT induced ROS overexpression and inhibited virulence factor expressions in MRSA. (a) ROS (reactive oxygen species) generation in MRSA exposed to TBPP (12 μM) for 20 min followed by irradiation with different doses (0, 20, 60 J cm^{-2}) of blue light was measured *via* 2,7-dichlorofluorescein diacetate (DCFH-DA, 10 μM) probe by flow cytometry. (b–e) Levels of superoxide anion, singlet oxygen, hydrogen peroxide and hydroxyl radical in TBPP (0, 0.5, 1, 2, 4, 8, 12 μM) solution after irradiation with blue light (445 nm; 0, 20, 60 J cm^{-2}) (mean ± SD, $n = 3$). Superoxide anion levels were determined by the product of azoic compound at 530 nm (b), singlet oxygen levels were tested by fluorescent probe SOSG (singlet oxygen sensor green; Ex: 504 nm, Em: 525 nm) (c), hydrogen peroxide levels were measured by absorbance at 570 nm using hydrogen peroxide assay kit (d), hydroxyl radical levels were detected by the absorbance (665 nm) changes of methylene blue [hydroxyl radical (OH^-) indicator] solution (e). ****$P < 0.0001$ (two-way ANOVA, Dunnett's *posthoc* test). (f and g) mRNA levels of agrA (accessory gene regulator A) and TSST-1 (toxic shock syndrome toxin 1) in MRSA treated with TBPP (12 μM, 20 min) + BL (60 J cm^{-2}) were tested by qPCR (mean ± SD, $n = 3$). 16S rRNA levels were utilized as the internal standard. ***$P < 0.001$ (two-way ANOVA, Dunnett's *posthoc* test). PDT, photodynamic therapy. BL, blue light. MRSA, methicillin-resistant *Staphylococcus aureus*.

found in the levels of the other three types of ROS, indicating that the ROS produced by TBPP + BL was mainly singlet oxygen.

The overexpression of ROS in bacteria is harmful to bacterial structures and functions. As shown in Fig. S8,† after treatments with TBPP + BL, the levels of ATP (adenosine triphosphate), which is the major source of energy for numerous significant biological processes, were drastically reduced, indicating the serious destruction of MRSA. *Staphylococcus aureus* (*S. aureus*) is capable of secreting diverse virulence factors to cause infection. Among the virulence determinants, accessory gene regulator A (agrA) is a vital regulatory factor that regulates virulence factors

production. And the superantigen toxic shock syndrome toxin 1 (TSST-1) serves as the principal contributor to toxic shock syndrome.[35,36] To explore the impacts of TBPP-PDT on MRSA virulence factors, the expressions of TSST-1 and agrA were tested by qPCR. As anticipated, the levels of agrA and TSST-1 mRNA in MRSA were decreased after treatments with TBPP + BL (Fig. 3f and g), suggesting that TBPP-PDT suppressed agrA and TSST-1 expressions. These results disclosed that TBPP-PDT could inhibit the factor expressions in relation to MRSA infection.

2.3 The evaluation of biofilm inhibition induced by TBPP-PDT

Biofilms are composed of the secretory extracellular polymeric substances and the encapsulated microbes. The formation of biofilms makes the bacteria encased in them insensitive to antibiotics and other environmental stresses, leading to severe bacterial infection.[37,38] To explore the impact of TBPP + BL on biofilm formation, MRSA were treated with TBPP + BL, and then the bacteria were cultured in culture plates to form biofilms. The biofilms were stained by crystal violet. As shown in Fig. S9,† slight crystal violet dye indicated the suppression of biofilm formation after treatments of TBPP + BL. Moreover, the mass of biofilms in TBPP + BL group was less compared with the biofilms in the control groups (Fig. S10†). These results suggested that TBPP-PDT had the capacity to suppress MRSA biofilm formation.

For investigating the bactericidal effects of TBPP + BL on the bacteria wrapped in mature biofilms, the vitality of MRSA in biofilms was measured by colony counting assay. As shown in Fig. 4a, MRSA vitality was obviously inhibited by the combined treatments of TBPP and BL. The results of live/dead assay showed that the red fluorescence enhanced gradually after TBPP + BL treatments (Fig. S11†), indicating that TBPP + BL could eliminate the MRSA embedded in biofilms. These results motivated us to evaluate the effects of TBPP + BL on the mature biofilm mass. As shown in Fig. 4b, TBPP together with BL markedly diminished MRSA biofilm mass. Furthermore, after the combined TBPP and BL treatments, bacterial adhesion determined by crystal violet staining was dramatically reduced (Fig. 4c). Correspondingly, the biofilm thickness was also reduced (Fig. 4d), which was stained with fluorescein diacetate (FDA) and determined by 3D confocal microscopy. These results indicated that TBPP-PDT could remove MRSA in biofilms and disperse the biofilms.

2.4 The assessment of biofilm elimination and wound healing induced by TBPP-PDT *in vivo*

Next, we examined the effects of TBPP-PDT on biofilm elimination *in vivo*. MRSA were injected to the wounds on the back of ICR mice for 2 days to construct biofilm infection model (Fig. 5a).[39] The wounds received treatments with PBS, BL alone, TBPP alone, TBPP + BL, respectively. As shown in Fig. 5b, the combined treatments of TBPP and BL remarkably inhibited skin wound infection and promoted the healing of wounds. However, the wounds treated with PBS, BL alone or TBPP alone presented erythema, swollen and suppuration. For evaluating wound-healing efficacy of TBPP + BL, the wound tissues were

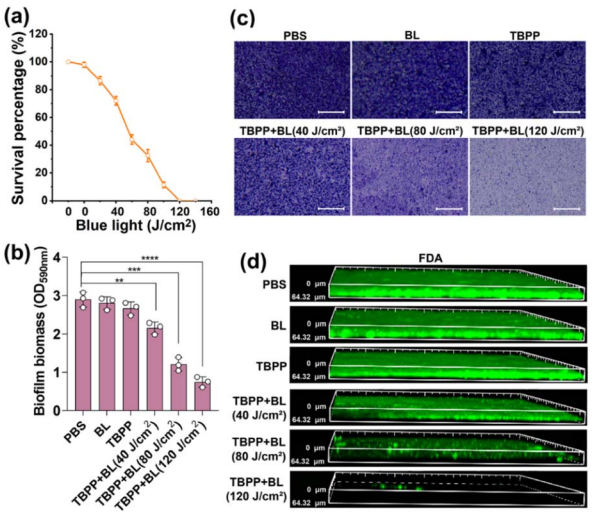

Fig. 4 TBPP-PDT eliminated MRSA from mature biofilms and disintegrated biofilms. (a) Quantification of MRSA in biofilms. 36 h old biofilms were treated with TBPP (12 μM) for 20 min followed by irradiation with different doses (0, 20, 40, 60, 80, 100, 120, 140 J cm^{-2}) of blue light. Then the bacteria in biofilms was quantified by colony counting assay (mean ± SD, $n = 3$). (b) Quantization of biofilms stained by crystal violet at 590 nm. MRSA biofilms (36 h old) were exposed to TBPP (12 μM) for 20 min followed by irradiation with different doses (0, 40, 80, 120 J cm^{-2}) of blue light (mean ± SD, $n = 3$). $^{**}P < 0.01$, $^{***}P < 0.001$, $^{****}P < 0.0001$ (two-way ANOVA, Dunnett's *posthoc* test). (c) Microscopic images of the biofilms stained by crystal violet. 36 h old MRSA biofilms were exposed to TBPP (12 μM) for 20 min followed by irradiation with different doses (0, 40, 80, 120 J cm^{-2}) of blue light. The biofilms were observed by microscope. Scale bar = 100 μm. (d) 3D confocal images of MRSA biofilms exposed to TBPP (12 μM) for 20 min followed by irradiation with different doses (0, 40, 80, 120 J cm^{-2}) of blue light. The biofilms were dyed with fluorescein diacetate (FDA). PDT, photodynamic therapy. BL, blue light. MRSA, methicillin-resistant *Staphylococcus aureus*.

stained with hematoxylin and eosin (H&E). As shown in Fig. 5c, intact epidermal layer was observed in the group treated with TBPP + BL. However, fragmentary epidermal layer was found in the control groups. To further evaluate antibacterial activity, the wound tissues were separated and the bacteria around the wounds were quantified. As shown in Fig. 5d and e, the MRSA population was dramatically inhibited by the combined treatments of TBPP and BL. The reduction of inflammatory factors indicated that TBPP + BL could inhibit inflammatory reaction around the wounds (Fig. S12†). Moreover, no remarkable injures or abnormalities appeared in the major organs of the mice after TBPP-PDT treatments (Fig. S13†), and TBPP-PDT did not induce perceptible erythema or edema in the skins of mice (Fig. S14†). In addition, no significant inhibition of NIH/3T3 cell viability, DNA damage or protein denaturation were observed after TBPP-PDT treatments (Fig. S15–17†). Therefore, TBPP-PDT showed excellent wound healing performance.

3 Discussion

Photosensitizers for photodynamic therapy (PDT) have been developed for three generations. The first generation of photosensitizers mainly includes hematoporphyrin derivatives and

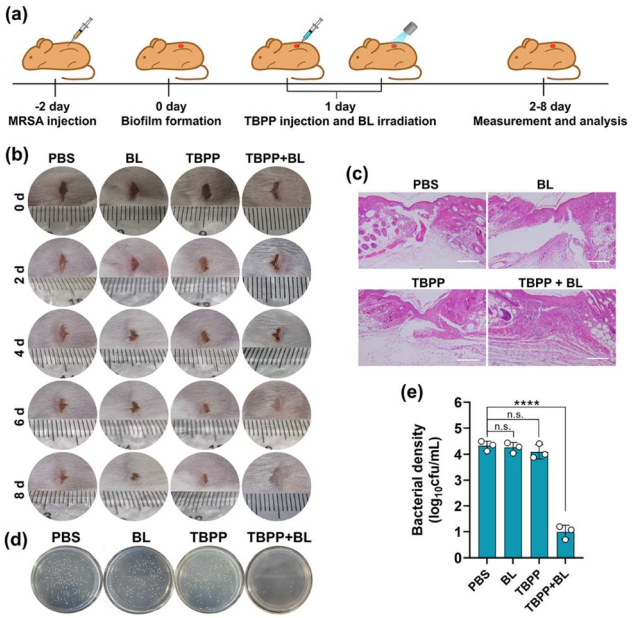

Fig. 5 TBPP-PDT eliminated biofilms from infected wounds and accelerated wound healing. (a) Schematic illustration of the experimental procedure for eliminating biofilms from infected mice. (b) Digital images of the wounds on mice in the therapeutic process. The mice were administered with PBS, blue light alone, TBPP alone (100 μL, 0.5 mg kg^{-1}), TBPP (100 μL, 0.5 mg kg^{-1}) + blue light (120 J cm^{-2}). The wounds were surveyed every two days. (c) Micrographs presenting section of skin tissues with H&E staining. (d) MRSA separated from the wounds were grown on LB agar dishes. (e) The count of the living MRSA in the wound tissues. Error bars are based on three mice per group (mean ± SD, $n = 3$). ****$P < 0.0001$ (two-way ANOVA, Dunnett's *posthoc* test). PDT, photodynamic therapy. BL, blue light. MRSA, methicillin-resistant *Staphylococcus aureus*.

photofrin. The second generation of photosensitizers consists of porphyrin derivatives and non-porphyrin compounds, and the second generation of photosensitizers linked to antibodies or other bioactive molecules such as liposomes and nucleotides for specific functions are known as the third generation of photosensitizers.[40] Thus, the development of second-generation photosensitizers is still the focus in PDT field. In the second generation of photosensitizers, porphyrin photosensitizers occupy the central position. At present, most clinically approved photosensitizers are porphyrin photosensitizers.[41] Moreover, many porphyrin photosensitizers are in the preclinical stages and undergoing clinical trials.[42] Therefore, porphyrin photosensitizers play important roles in photodynamic therapy. In this work, the photodynamic bactericidal functions of five porphyrin derivatives against drug-resistant bacteria were studied, and TBPP-PDT showed outstanding bactericidal effects. As a derivative of porphyrin, TBPP has great potential to be developed as a photosensitizer for clinical treatments against drug-resistant bacteria.

Biofilms refer to the communities of microorganisms and self-generated extracellular matrix, which adhered to a surface or interphase.[43] The initial phase of biofilm formation is the adhesion of bacteria to a surface, followed by the division of bacteria to constitute microcolonies and the generation of the extracellular matrix, which including polysaccharides, nucleic acids, lipids proteins.[44] After the maturation of biofilms, the bacteria wrapped in biofilms are protected from environmental stressors, such as desiccation, immune system attack, protozoa ingestion and antimicrobials.[45] Many serious bacterial infections are related with biofilms, such as chronic pneumonia, ear and wound infections. More than 80 percent of microbial infections have a connection with biofilms, and such infections are extremely difficult to treat.[46] Therefore, inhibiting biofilm formation or decomposing mature biofilms are the important goals of antibacterial drug developments. Our results showed that TBPP-PDT could effectively suppress biofilm formation and disintegrate mature biofilms partly, suggesting its great potential to be developed as an antibiofilm strategy.

According to our data, TBPP was able to enter the bacterial cells. Moreover, after the combined treatments of TBPP and BL, the cell membrane of MRSA was obviously destroyed. Therefore, the destruction of the cell membrane may be a dual action of both extracellular ROS and intracellular ROS. Our results showed that ATP levels decreased after the treatments of TBPP + BL, suggesting that intracellular ROS also disrupted energy metabolism.

The infectious ability of *Staphylococcus aureus* (*S. aureus*) and its success as a pathogen are associated with virulence factor expression. As the response regulator of the two-component signal transduction system (TCST) of *S. aureus*, accessory gene regulator A (agrA) can regulate the expression of bacterial virulence factors and plays important roles in the pathogenic process of *S. aureus*.[47] Toxic shock syndrome toxin 1 (TSST-1) is a significant virulence factor of *S. aureus* and brings about toxic shock syndrome (TSS) that can be identified by rash, fever, hypotension, organ damage, resulting in a high mortality rate.[48] Our results exhibited that the expressions of agrA and TSST-1 were down-regulated, indicating that TBPP-PDT could inhibit the infection and pathogenic capacity of MRSA.

4 Experimental

4.1 Bacterial culture and bactericidal activity against planktonic cells

MRSA monocolony was moved to 20 mL liquid LB (Luria–Bertani) culture medium and cultivated for 12 h while shaking (37 °C). In the experiments of antibacterial activity of photoexcited compounds, the MRSA were attenuated with culture medium to 10^6 cfu (colony forming units) mL^{-1}. Then compounds with varying concentrations were respectively blended with MRSA solution and incubated for 20 min. Finally, 445 nm and 420 nm lasers (Viasho, China) with different power densities was used as the blue light source. The antibacterial activities of TPP-PDT, TBPP-PDT, TCPP-PDT, TFPP-PDT were activated by 445 nm laser, and the antibacterial activities of TIPP-PDT were activated by 420 nm laser. The bactericidal effects of blue light alone or compound alone were also assessed. After irradiation for the indicated light doses, the MRSA solution was put on LB agar plates to calculate the number of living bacteria. The light doses were calculated by multiplying power density (0.2 W cm^{-2}) by irradiation times (second). 20 J cm^{-2}: 0.2 W cm^{-2}, 100 s; 40 J cm^{-2}: 0.2 W cm^{-2}, 200 s; 60 J cm^{-2}: 0.2 W cm^{-2}, 300 s; 80 J

cm^{-2}: 0.2 W cm^{-2}, 400 s; 100 J cm^{-2}: 0.2 W cm^{-2}, 500 s; 120 J cm^{-2}: 0.2 W cm^{-2}, 600 s.

4.2 Membrane potential analysis

The changes of bacterial membrane potential were examined by using membrane potential sensitive fluorochrome, DiBAC4(3) [bis-(1,3-dibutylbarbituric acid)-trimethine oxonol].[49] After treatments with TBPP (12 μM, 20 min) and 445 nm laser irradiation (0, 20, 60 J cm^{-2}), the MRSA cells were collected. Then, 100 μL of collected cell suspensions were placed in black 96-well plates for 30 min at 37 °C. 1 μL of the fluorescent probe DiBAC4(3) was added and kept at 37 °C for 30 min. Finally, fluorescence was determined (Ex: 492 nm, Em: 515 nm) by using a fluorescence microplate reader (Varioskan LUX, Thermo Fisher, USA).

4.3 Live/dead assay (SYTO9/PI staining)

After treatments, MRSA were collected, stained by SYTO9 (3.34 μM) and propidium iodide (PI, 20 μM) for 15 min under light-shielding, and imaged using a confocal microscopy (Nikon C2, Japan).

4.4 Reactive oxygen species (ROS) detection

ROS generation in bacterial cells was tested using an oxidation sensitive dye 2,7-dichlorofluorescein diacetate (DCFH-DA, R272916, Aladdin, China).[50] MRSA were exposed to TBPP (12 μM) for 20 min followed by irradiation with different doses (0, 20, 60 J cm^{-2}) of blue light, then the bacteria were mixed with DCFH-DA (10 μM) and maintained for 20 min under light-shielding. The generation of ROS was detected by flow cytometry (NovoCyte, Agilent, USA) and fluorescence microscope (Axio Scope5, ZEISS, Germany).

4.5 Superoxide anion ($O_2^{\cdot -}$), singlet oxygen ($^1O_2$), hydrogen peroxide (H_2O_2) and hydroxyl radical (OH^-) detection

4.5.1 Superoxide anion ($O_2^{\cdot -}$) detection. Different concentrations of TBPP (0, 0.5, 1, 2, 4, 8, 12 μM) solutions were irradiated with blue light (445 nm; 0, 20, 60 J cm^{-2}). The superoxide anion level in the solution was determined using Superoxide Anion Content Assay Kit (BC1290, Solarbio) and UV-Vis spectrophotometer (UV-3600i Plus, Shimadzu, Japan) at the wavelength of 530 nm.

4.5.2 Singlet oxygen ($^1O_2$) detection. Singlet oxygen fluorescent probe SOSG (singlet oxygen sensor green) was dissolved in methyl alcohol at the concentration of 5 mM in the dark.[51] Different concentrations of TBPP (0, 0.5, 1, 2, 4, 8, 12 μM) solution were mixed with SOSG (10 μM) solution, and irradiated with blue light (445 nm; 0, 20, 60 J cm^{-2}). The solution was analyzed with fluorescence (Ex: 504 nm, Em: 525 nm) using fluorescence spectrophotometer (FLS1000, Edinburgh Instruments, UK).

4.5.3 Hydrogen peroxide (H_2O_2) detection. Different concentrations of TBPP (0, 0.5, 1, 2, 4, 8, 12 μM) solutions were irradiated with blue light (445 nm; 0, 20, 60 J cm^{-2}). The hydrogen peroxide level in the solution was determined using Hydrogen Peroxide Assay Kit (S0038, Beyotime Biotechnology) and UV-Vis spectrophotometer (UV-3600i Plus, Shimadzu, Japan) at the wavelength of 570 nm.

4.5.4 Hydroxyl radical (OH^-) detection. The hydroxyl radical indicator methylene blue [MB, 3,7-bis(dimethylamino)-phenothiazin-5-ium chloride] was dissolved in DMSO at the concentration of 10 mM. A range of concentrations of TBPP (0, 0.5, 1, 2, 4, 8, 12 μM) solution were mixed with MB solution (40 μM, 1 mL), irradiated with blue light (445 nm; 0, 20, 60 J cm^{-2}), and the solution was collected. The absorbance of MB was detected (665 nm) by UV-Vis spectrophotometer.

4.6 Biofilm formation and crystal violet staining assay

MRSA were inoculated into liquid LB medium and cultivated overnight at 37 °C and 180 rpm. A diluted MRSA solution was plated in 24-well plates with glass flat bottom and cultured for 36 h at 37 °C for biofilm formation. Removed the old medium and added fresh medium each 24 h. For removing unbound bacteria, each of the wells was rinsed with aseptic PBS buffer. Crystal violet solution (0.1%, 500 μL) was put into the biofilms and kept in incubation for 10 min. Removed the solution and rinsed with PBS buffer. The images were acquired using optical microscope.

To quantify the biofilms, the biofilms grew in 24 well plates with glass flat-bottoms were washed with PBS for 3 times. 500 μL of glutaraldehyde solution (2.5%) was added for fixation for 10 min. Then the biofilms were rinsed with PBS. 500 μL 0.1% crystal violet was added and maintained in incubation for 10 min. Crystal violet solution was removed, washed with PBS and air-dried. Then acetic acid (30%, 500 μL) was added for dissolving dye for 30 min. 100 μL of the dye solution was tested by optical density at 590 nm using a plate reader (Epoch2, BioTeK, Germany).[52]

4.7 Enzyme-linked immunosorbent assay (ELISA)

Tumor necrosis factor α (TNF-α) as well as interleukin 6 (IL-6) levels around the wounds were detected by ELISA. ELISA assay kits (EM0183 and EM0121) were purchased from Fine Biotech (Wuhan, China), and all procedures followed the manufacturer's instructions.

4.8 Haematoxylin and eosin (H&E) staining analysis

Immediately after surgical removal, wound tissues and organs (liver, spleen, kidney, heart and lung) were fixed overnight in paraformaldehyde (4%), immersed in paraffin, sectioned (4 μm thick) and stained by hematoxylin and eosin. The histological sections of the wound tissues and organs were inspected through microscope.

5 Conclusions

In conclusion, five porphyrin derivatives (TPP, TBPP, TCPP, TFPP, TIPP) were evaluated for photodynamic microbicidal effects to overcome the problems of drug resistance. The results showed that TBPP mediated PDT presented the most prominent bactericidal effects against MRSA (Fig. S18†). Further studies showed that TBPP together BL could injure cell membrane

integrity, inhibit ATP synthesis and virulence factor expression *via* ROS overexpression in bacterial cells, resulting in MRSA death. Interestingly, the combined treatments of TBPP and BL suppressed biofilm formation capacity of MRSA. Moreover, TBPP + BL had the ability to eradicate MRSA embedded in biofilms and disintegrate the mature biofilms. What's more, TBPP-PDT could eliminate MRSA and biofilms from the wounds in mice and reduce inflammatory response of infected skin tissues, leading to wound healing acceleration *in vivo*. Therefore, TBPP has great potential as a BL photosensitizer for the treatments of skin infections induced by drug-resistant bacteria.

Ethical statement

All the mice (male ICR mice weighted about 20.0 g) used in this study were purchased from Shanxi Medical University (Shanxi, China). All *in vivo* experiments were approved by the Animal Ethics Committee of Shanxi Medical University. All animal procedures were in accord with the guidelines of the Institutional Animal Care and Use Committee of Shanxi Medical University (Shanxi, China). The mice were housed in a temperature-controlled, ventilated and standardized disinfected animal room, and allowed to acclimatize for 1 week before the start of experiments.

Data availability

The data supporting this article have been included as part of the ESI.†

Author contributions

Hongshuang Qin, Tao Liu and Chuanqi Zhao designed research. Huaying Niu, Yanxiang Guo and Xiaoting Wang performed the experiments. Hongshuang Qin, Huaying Niu and Yanxiang Guo analyzed the data. All authors wrote and revised the manuscript.

Conflicts of interest

There are no conflicts to declare.

Acknowledgements

This work was supported by the Basic Research Project of Shanxi Province (202303021211336, 202203021221228), the Jilin Province Science and Technology Development Plan Project (20210101130JC), the National Natural Science Foundation of China (22122704, 22377120), the Key Research Program of Lvliang City (2022SHFZ39, 2023GXYF04, 2024GX14) and the Shanxi Province Higher Education Reform and Innovation Project (J20241416, J20241417).

Notes and references

1 U. Theuretzbacher, S. Gottwalt, P. Beyer, M. Butler, L. Czaplewski, C. Lienhardt, L. Moja, M. Paul, S. Paulin, J. H. Rex, L. L. Silver, M. Spigelman, G. E. Thwaites, J. P. Paccaud and S. Harbarth, *Lancet Infect. Dis.*, 2019, **19**, e40–e50.
2 N. Hanna, A. J. Tamhankar and C. Stålsby Lundborg, *Lancet Planet. Health*, 2023, **7**, e45–e54.
3 P. Piewngam, S. Khongthong, N. Roekngam, Y. Theapparat, S. Sunpaweravong, D. Faroongsarng and M. Otto, *Lancet Microbe*, 2023, **4**, e75–e83.
4 M. Bassetti, F. Magnè, D. R. Giacobbe, L. Bini and A. Vena, *Eur. Respir. Rev.*, 2022, **31**, 220119.
5 S. Deo, K. L. Turton, T. Kainth, A. Kumar and H. J. Wieden, *Biotechnol. Adv.*, 2022, **59**, 107968.
6 A. Upadhayay, J. Ling, D. Pal, Y. Xie, F. F. Ping and A. Kumar, *Drug Resistance Updates*, 2023, **66**, 100890.
7 O. Ayobami, S. Brinkwirth, T. Eckmanns and R. Markwart, *Emerging Microbes Infect.*, 2022, **11**, 443–451.
8 A. Burke, M. Di Filippo, S. Spiccio, A. M. Schito, D. Caviglia, C. Brullo and M. Baumann, *Int. J. Mol. Sci.*, 2023, **24**, 5319.
9 A. S. Lee, H. de Lencastre, J. Garau, J. Kluytmans, S. Malhotra-Kumar, A. Peschel and S. Harbarth, *Nat. Rev. Dis. Primers*, 2018, **4**, 18033.
10 Y. Sun, H. Qin, Z. Yan, C. Zhao, J. Ren and X. Qu, *Adv. Funct. Mater.*, 2019, **29**, 1808222.
11 H. H. Buzzá, F. Alves, A. J. B. Tomé, J. Chen, G. Kassab, J. Bu, V. S. Bagnato, G. Zheng and C. Kurachi, *Proc. Natl. Acad. Sci. U. S. A.*, 2022, **119**, e2216239119.
12 T. Cui, S. Wu, Y. Sun, J. Ren and X. Qu, *Nano Lett.*, 2020, **20**, 7350–7358.
13 L. Yang, D. Zhang, W. Li, H. Lin, C. Ding, Q. Liu, L. Wang, Z. Li, L. Mei, H. Chen, Y. Zhao and X. Zeng, *Nat. Commun.*, 2023, **14**, 7658.
14 Z. Wang, A. Wu, W. Cheng, Y. Li, D. Li, L. Wang, X. Zhang and Y. Xiao, *Nat. Commun.*, 2023, **14**, 7251.
15 A. Taninaka, H. Kurokawa, M. Kamiyanagi, T. Ochiai, Y. Arashida, O. Takeuchi, H. Matsui and H. Shigekawa, *Commun. Biol.*, 2023, **6**, 1212.
16 W. Zhu, Y. Li, S. Guo, W. J. Guo, T. Peng, H. Li, B. Liu, H. Q. Peng and B. Z. Tang, *Nat. Commun.*, 2022, **13**, 7046.
17 F. Vatansever, W. C. de Melo, P. Avci, D. Vecchio, M. Sadasivam, A. Gupta, R. Chandran, M. Karimi, N. A. Parizotto, R. Yin, G. P. Tegos and M. R. Hamblin, *FEMS Microbiol. Rev.*, 2013, **37**, 955–989.
18 E. C. Ziegelhoffer and T. J. Donohue, *Nat. Rev. Microbiol.*, 2009, **7**, 856–863.
19 F. D. Halstead, J. E. Thwaite, R. Burt, T. R. Laws, M. Raguse, R. Moeller, M. A. Webber and B. A. Oppenheim, *Appl. Environ. Microbiol.*, 2016, **82**, 4006–4016.
20 Y. Zhang, Y. Zhu, A. Gupta, Y. Huang, C. K. Murray, M. S. Vrahas, M. E. Sherwood, D. G. Baer, M. R. Hamblin and T. Dai, *J. Infect. Dis.*, 2014, **209**, 1963–1971.
21 M. Lu, S. Wang, T. Wang, S. Hu, B. Bhayana, M. Ishii, Y. Kong, Y. Cai, T. Dai, W. Cui and M. X. Wu, *Sci. Transl. Med.*, 2021, **13**, 3571.
22 I. Ahmed, Y. Fang, M. Lu, Q. Yan, A. El-Hussein, M. R. Hamblin and T. Dai, *Recent Pat. Anti-Infect. Drug Discovery*, 2018, **13**, 70–88.

23 R. Akasov, E. V. Khaydukov, M. Yamada, A. V. Zvyagin, A. Leelahavanichkul, L. G. Leanse, T. Dai and T. Prow, *Adv. Drug Deliv. Rev.*, 2022, **184**, 114198.
24 M. Schreiner, W. Bäumler, D. B. Eckl, A. Späth, B. König and A. Eichner, *Br. J. Dermatol.*, 2018, **179**, 1358–1367.
25 R. McDonald, S. J. Macgregor, J. G. Anderson, M. Maclean and M. H. Grant, *J. Biomed. Opt.*, 2011, **16**, 048003.
26 M. M. Kleinpenning, T. Smits, M. H. Frunt, P. E. van Erp, P. C. van de Kerkhof and R. M. Gerritsen, *Photodermatol. Photoimmunol. Photomed.*, 2010, **26**, 16–21.
27 M. A. Rajora, J. W. H. Lou and G. Zheng, *Chem. Soc. Rev.*, 2017, **46**, 6433–6469.
28 A. E. O'Connor, W. M. Gallagher and A. T. Byrne, *Photochem. Photobiol.*, 2009, **85**, 1053–1074.
29 A. Arlegui, Z. El-Hachemi, J. Crusats and A. Moyano, *Molecules*, 2018, **23**, 3363.
30 M. Novoa-Cid, A. Melillo, B. Ferrer, M. Alvaro and H. G. Baldovi, *Nanomaterials*, 2022, **12**, 3197.
31 P. Dechan and G. D. Bajju, *ACS Omega*, 2020, **5**, 17775–17786.
32 D. Sen, P. Błoński, B. de la Torre, P. Jelínek and M. Otyepka, *Nanoscale Adv.*, 2020, **2**, 2986–2991.
33 S. Lakhundi and K. Zhang, *Clin. Microbiol. Rev.*, 2018, **31**, e00020.
34 S. A. Tursi, R. D. Puligedda, P. Szabo, L. K. Nicastro, A. L. Miller, C. Qiu, S. Gallucci, N. R. Relkin, B. A. Buttaro, S. K. Dessain and Ç. Tükel, *Nat. Commun.*, 2020, **11**, 1007.
35 B. R. Boles and A. R. Horswill, *PLoS Pathog.*, 2008, **4**, e1000052.
36 T. Yamaguchi, K. Furuno, K. Komori, T. Abe, T. Sato, S. Ogihara, K. Aoki, Y. Ishii and K. Tateda, *Clin. Microbiol. Infect.*, 2024, **30**, 779–786.
37 Y. Bordon, *Nat. Rev. Immunol.*, 2023, **23**, 474.
38 M. Maree, L. T. Thi Nguyen, R. L. Ohniwa, M. Higashide, T. Msadek and K. Morikawa, *Nat. Commun.*, 2022, **13**, 2477.
39 W. Xiu, L. Wan, K. Yang, X. Li, L. Yuwen, H. Dong, Y. Mou, D. Yang and L. Wang, *Nat. Commun.*, 2022, **13**, 3875.
40 U. Chilakamarthi and L. Giribabu, *Chem. Rec.*, 2017, **17**, 775–802.
41 M. C. S. Vallejo, N. M. M. Moura, A. Gomes, A. S. M. Joaquinito, M. A. F. Faustino, A. Almeida, I. Gonçalves, V. V. Serra and M. Neves, *Int. J. Mol. Sci.*, 2021, **22**, 4121.
42 S. S. Lucky, K. C. Soo and Y. Zhang, *Chem. Rev.*, 2015, **115**, 1990–2042.
43 A. Zhang, H. Wu, X. Chen, Z. Chen, Y. Pan, W. Qu, H. Hao, D. Chen and S. Xie, *Sci. Adv.*, 2023, **9**, eadg9116.
44 L. Karygianni, Z. Ren, H. Koo and T. Thurnheer, *Trends Microbiol.*, 2020, **28**, 668–681.
45 H. C. Flemming, E. D. van Hullebusch, T. R. Neu, P. H. Nielsen, T. Seviour, P. Stoodley, J. Wingender and S. Wuertz, *Nat. Rev. Microbiol.*, 2023, **21**, 70–86.
46 R. Roy, M. Tiwari, G. Donelli and V. Tiwari, *Virulence*, 2018, **9**, 522–554.
47 C. Leseigneur, L. Boucontet, M. Duchateau, J. Pizarro-Cerda, M. Matondo, E. Colucci-Guyon and O. Dussurget, *eLife*, 2022, **11**, e79941.
48 P. M. Schlievert and C. C. Davis, *Clin. Microbiol. Rev.*, 2020, **33**, e00032.
49 F. David, A. Berger, R. Hänsch, M. Rohde and E. Franco-Lara, *Microb. Cell Fact.*, 2011, **10**, 23.
50 F. Akhtar, A. U. Khan, L. Misba, K. Akhtar and A. Ali, *Eur. J. Pharm. Biopharm.*, 2021, **160**, 65–76.
51 H. B. Cheng, B. Qiao, H. Li, J. Cao, Y. Luo, K. M. Kotraiah Swamy, J. Zhao, Z. Wang, J. Y. Lee, X. J. Liang and J. Yoon, *J. Am. Chem. Soc.*, 2021, **143**, 2413–2422.
52 R. Waldrop, A. McLaren, F. Calara and R. McLemore, *Clin. Orthop. Relat. Res.*, 2014, **472**, 3305–3310.